Ground Resistance and Impulse Impedance Measurements: Results and Major Error Factors

Adroaldo Raizer
Federal University of Santa Catarina
UFSC
Florianópolis, Brazil
adroaldo.raizer@gmail.com

Vilson Luiz Coelho
Faculty SATC
FASATC
Criciúma, Brazil
vilson.coelho@vlc.eng.br

Thiago Schmoeller
Federal University of Santa Catarina
UFSC
Florianópolis, Brazil
eng.thiagoschmoeller@gmail.com

***Abstract* — This paper presents results of field measurements of ground resistance and impulse impedance in experimental ground grids. Following the recommended measurement methodologies and with possession of the necessary equipment, a set of data was obtained that allowed the identification of important factors that influence the results of the measurements and can insert significant errors.**

Keywords — Field Measurements, Grounding, Ground Grids, Ground Resistance, Impulse Impedance.

I. INTRODUCTION

The existence of a path of low impedance to the ground, to drain the currents of the surges and to control the generated surges, is one of the determinant and indispensable factors in the analysis of electrical safety.

In environments subject to atmospheric discharges, the simple evaluation of the ground resistance of the system (R_{LF}) is not enough to validate the effectiveness of it, when submitted to this electromagnetic phenomenon. For proper sizing of an effective system for these types of surges, it is necessary to evaluate the transient impedance *Z(t)* or impulse impedance ($Z_P=V_{max}/I_{max}$). Only with this data, it is possible to determine the overvoltages produced during a surge, and to assess the performance of the system for safety and availability requirements [1, 2].

However, the determination of the impulse impedance Z_P of a system is not easily obtained: it is necessary to apply an appropriate methodology, considering special precautions to mitigate interferences and couplings, as well as adequate equipment, capable of simulating the surges and capture the data during the field tests.

As a result, this paper presents a series of ground resistance and impulse impedance field measurements under various conditions:

- Two different experimental grounding grids: 5 m x 5 m e 10 m x 10 m;
- Auxiliary electrodes of voltage (*dP*) and current (*dA*) arranged in the same direction and in orthogonal position;
- Different distances between the current electrodes (*dA)* and the grids, varying from 0.75 times the diagonal (*D*) of the grid to 5*D*;
- Different distances between the voltage electrodes (*dP)* and the grids, varying from 10% to 90% of *dA.*

After the field tests, a set of data was obtained that indicated the need of special precautions in the performance of impedance measurements, under penalty of obtaining values with high error percentages.

II. THEORETICAL BASIS

The Fall-of-Potential Method, one of the most used for the measurement of ground resistance and ground impedance, is based on measurement of voltage between the grounding system and the auxiliary voltage electrode, which results from the current flow between the grounding system and the electrode auxiliary of current [3].

For ground resistance measurements, the equipment used is an earth meter. Considering that it has a low frequency voltage source, the capacitive and inductive components present in the grounding system are disregarded [4].

For a correct measurement, the distance *dA* of the auxiliary current electrode shall be four to ten times the largest diagonal *D* of the grounding system under measurement. The direction of the voltage electrode *dP* is optional: it can be in the same direction as the auxiliary current electrode, measuring the voltage *V1*, or in the opposite direction, by measuring the voltage *V2*. In both cases, the distance *dP* shall be 62% of *dA* for the correct measurement of the resistance *R* or transient impedance *Z(t)* of the grounding system [5, 6].

By varying the auxiliary voltage electrode in the same direction as the auxiliary current electrode, and using the ratio

$R=V1/I$, the typical curve of the system ground resistance is obtained, as shown in the solid line in the Fig. 1. When the measurement is performed with the auxiliary electrodes positioned orthogonally, the curve of the ground resistance, obtained by the ratio $R=V2/I$, is showed the dashed line response of Fig. 1 [5].

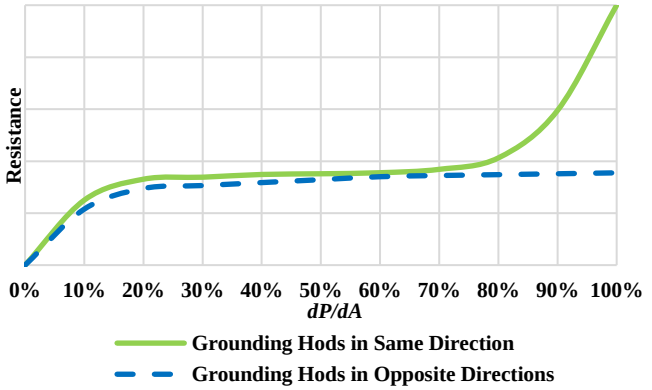

Fig. 1. Typical ground resistance measurement curve for auxiliary electrodes in the same direction and in opposite directions [5].

For the case of the transient impedance *Z(t)* measurement, the distance requirements between auxiliary electrodes and the grounding system under measurement are the same: the distance *dA* must be four to ten times the largest diagonal *D* of the system, and distance *dP* shall be 62% of *dA*. The difference is in the source that excites the system and in the equipment that read the voltage *v(t)* and current *i(t)* waveforms [5].

The source that excites the system is known as surge generator: a voltage source with extremely fast wavefront time, similar to the wavefront times of an atmospheric discharge, standardized by IEC 61000-4-5 [7]. For the capture of the voltage *v(t)* and current *i(t)* waveforms injected by the surge generator, it is necessary to use an oscilloscope with the appropriate voltage and current probes [5]. Applying these concepts in the field, it is possible to capture the transient impedance *Z(t)* of a grounding system, and obtain the impulse impedance values Z_P, defined as the ratio between the maximum voltage (V_{max}) and the maximum current (I_{max}) during the application of an surge, regardless of the instant of time in which they occur.

III. Methodology of Field Measurements

A. Characteristics of grounding grids and auxiliary voltage and current electrodes

The grounding grids used in this study are installed at the *Fazenda Experimental of UFSC* (Federal University of Santa Catarina), at coordinates 27°40'53"S and 48°32'12"W. They have two distinct sizes (5 m x 5 m and 10 m x 10 m), buried at 0.5 m depth, with copper conductors naked of 95 mm² [8].

At this same site, there are two more grounding grids, with similar geometry, and with different size (10 m x 5 m and 10 m x 2.5 m), which were not used in this study because of the proximity to each other. The 10 m x 10 m and 5 m x 5 m grids are distanced enough to mitigate any type of coupling or interference from one grid to the other.

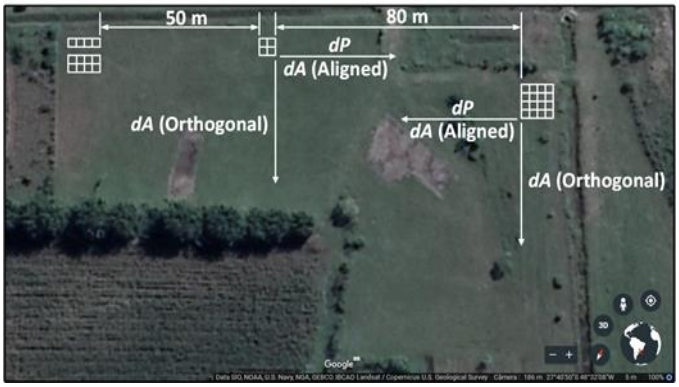

Fig. 2. Arrangement of the ground grids and the auxiliary voltage electrodes *dP* and current *dA* [9].

Based on the Fall-of-Potential Method, the following parameters were established for ground resistance and impedance measurements:

- Auxiliary current electrode *dA* equal to 0.75*D*, 1*D*, 2*D*, 3*D*, 4*D* e 5*D*, where *D* represents the largest diagonal of the grounding grid;
- Auxiliary electrode of voltage *dP* ranging from 10% to 90% of *dA*, in steps of 10%;
- Auxiliary electrodes *dA* and *dP* arranged in two directions (aligned and orthogonal), according to Fig. 2.

Measurements with auxiliary electrodes in the same direction were performed on January 6 and 7, 2018, on a sunny day, with temperatures between 30° C and 35 °C. Moreover, measurements with auxiliary electrodes arranged in orthogonal were performed on August 18, 2018, also on a sunny day with temperatures between 20 ºC and 25 ºC.

B. Equipment used

For the ground resistance measurements, the earth meter used was the Megabras MTD-20KWe [10]. For impedance measurements, was used a portable surge generator set to 2 kV with no load, Tektronix DPO3014 oscilloscope [11], Tektronix P6015A high voltage probe [12], and Tektronix TCP0020 current probe [13]. The assembled workbench is shown in Fig. 3.

Fig. 3. Resistance and impedance measurement workbench.

The auxiliary voltage electrode is composed of a vertical ground rod of 5/8", buried at a depth of 0.5 m. The auxiliary current electrode is composed of three 5/8" vertical ground rods, buried at 1 m depth, and spaced 1.5 m apart, forming an equilateral triangle.

The conductors from equipment to the auxiliary electrodes are composed of 2.5 mm² copper cables with PVC insulation 750 V. It was chosen to use cables instead of tapes, aluminum or copper, due to the large number of field measurements to be performed. To guarantee the spacing between electrodes and soil, wooden supports with plastic insulator were used.

C. Problems found during field measurements

1) High voltage probe positioning:

Due to the ease of installation, the first configuration of the test bench predicted that the voltage probe would stay on the bench. However, during the analysis of the captured data, values that did not correspond to the expected behavior were observed, presenting rapid peaks after the beginning of the stabilization of the tension curve, as shown in Fig. 4.

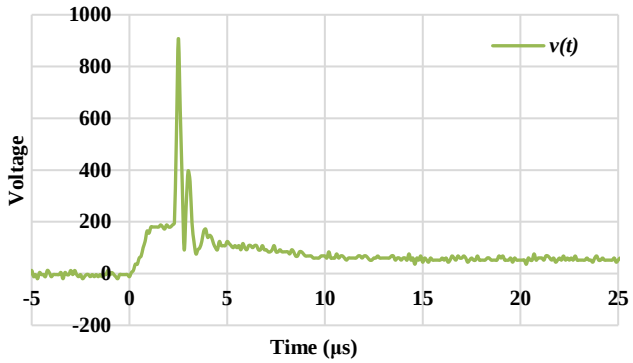

Fig. 4. Voltage waveform *v(t)* with peaks after stabilization begins.

To solve this problem, the high voltage probe was connected directly to the conductors of the ground grid.

2) Inductive coupling between the conductors of the voltage and current auxiliary electrodes:

The effect of the inductive coupling between the conductors of the voltage and current auxiliary electrodes, already known in the literature [5, 14], was relevant and considerable during the analysis of the results obtained in the field. Although this effect is already known, the verification of it during the analysis of field results did not occur in a trivial way.

The existence of this effect was characterized by the deformation of the voltage waveform *v(t)* in the measurements with auxiliary electrodes in the same direction, what presented a rapid and intense peak in the moment of the surge, as Fig. 5.

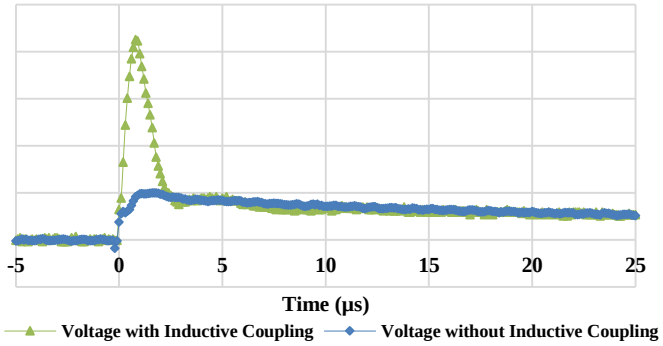

Fig. 5. Voltage waveform *v(t)* with and without coupling.

To obtain measurements without the effect of inductive coupling, the use of the *dP* voltage and *dA* current electrodes positioned orthogonally (90 degrees apart) proved to be an effective solution to mitigate this effect.

3) Power sources and remote ground reference:

The initial setup predicted the power to the oscilloscope and surge generator provided by a 12 Vdc / 220 Vca inverter, connected to a 12 Vdc battery. This configuration resulted in a short circuit between the auxiliary current electrode *dA* and the auxiliary voltage electrode *dP*, through the equipment ground pins (dashed line Fig. 6), which causes the oscilloscope to capture the output voltage of the surges generator.

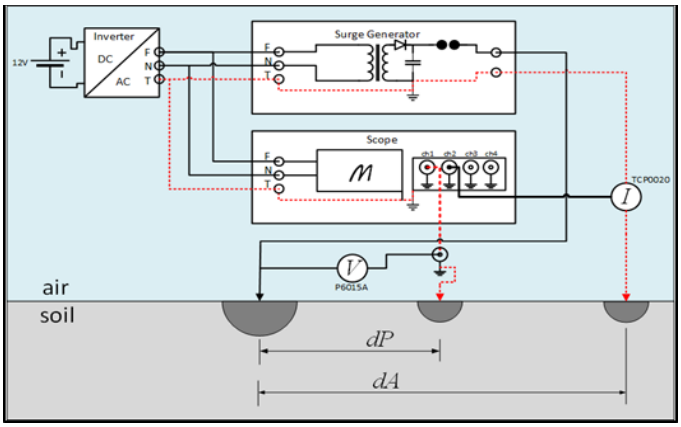

Fig. 6. Diagram of the short circuit between auxiliary voltage *dP* and current *dA* electrodes.

After consultation and analysis of ANSI / IEEE Std 81, and study of the equipment connection layout, it was concluded that it would be possible to supply the surge generator from a non-isolated source if the power supply to the measuring instrument was isolated. Thus, the surge generator has become to be powered by the distribution network of the local utility, and the battery inverter has become feeding the oscilloscope exclusively.

IV. Results of Field Measurements

In this chapter, results of the field tests are presented. It begins with the presentation of the results of the field measurements with electrodes in the same direction (subitems A and B), and then the results are presented for electrodes in orthogonal position (subitems C and D). At the end of the chapter, the results obtained (subitem E) are discussed.

A. Impulse impedance (Z_P) and ground resistance (R_{LF}) for 5 m x 5 m grid with auxiliary electrodes in the same direction

Fig. 7 shows, by way of illustration, a voltage *v(t)* and current *i(t)* waveforms captured when *dA* = 5*D* e *dP* = 0.6 *dA*. Fig. 8 shows the impulse impedance (Z_P) values.

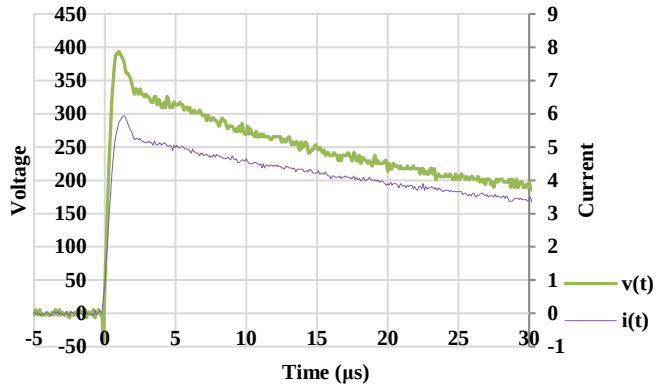

Fig. 7. Voltage *v(t)* and current *i(t)* waveforms for 5 m x 5 m grid, *dA* = 5*D* e *dP* = 0.6 *dA*.

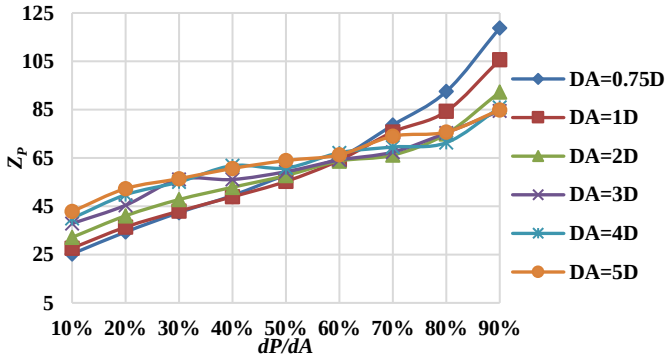

Fig. 8. Impulse impedance Z_P, 5 m x 5 m grid auxiliary electrodes in the same direction.

In this same measurement setup, Fig. 9 shows the ground resistance values (R_{LF}).

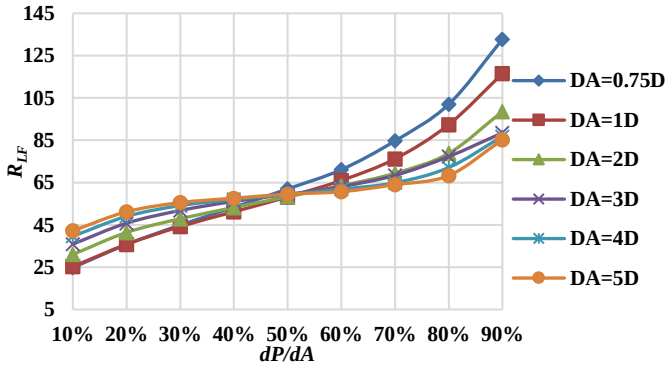

Fig. 9. Ground resistance R_{LF}, 5 m x 5 m grid, auxiliary electrodes in the same direction.

B. Impulse impedance (Z_P) and ground resistance (R_{LF}) for 10 m x 10 m grid with auxiliary electrodes in the same direction

Fig. 10 shows, by way of illustration, a voltage *v(t)* and current *i(t)* waveforms captured when *dA* = 5*D* e *dP* = 0.6 *dA*. Fig. 11 shows the impulse impedance (Z_P) values.

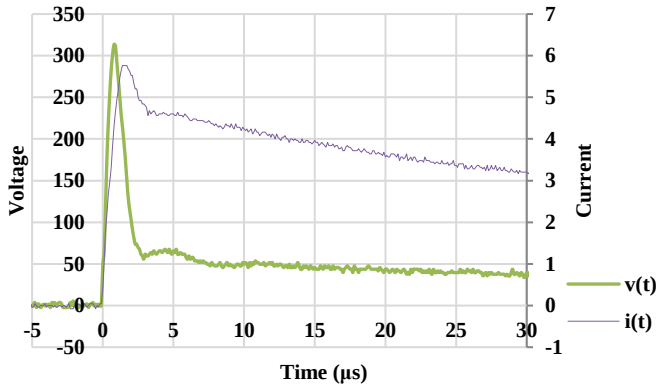

Fig. 10. Voltage *v(t)* and current *i(t)* waveforms for 10 m x 10 m grid, *dA* = 5*D* e *dP* = 0.6 *dA*.

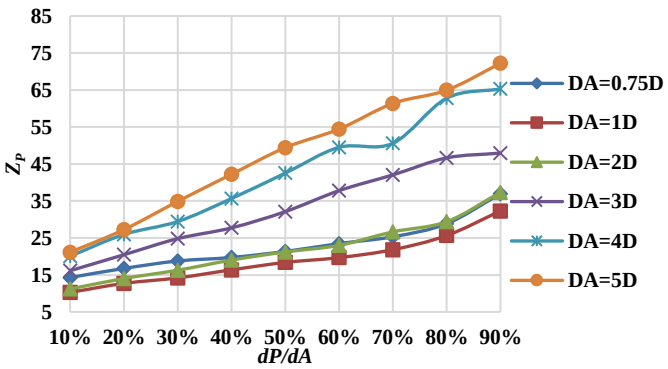

Fig. 11. Impulse impedance Z_P, 10 m x 10 m grid auxiliary electrodes in the same direction.

In this same measurement setup, Fig. 12 shows the ground resistance values (R_{LF}).

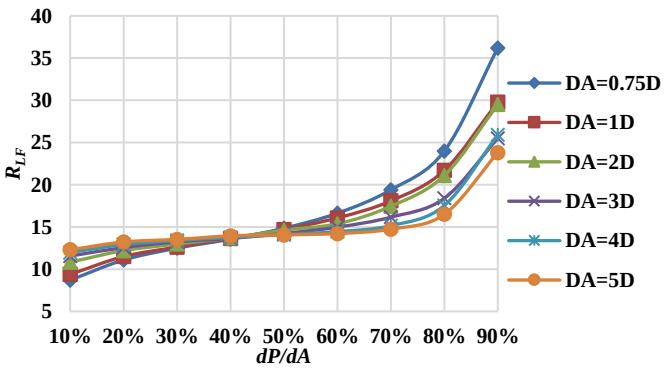

Fig. 12. Ground resistance R_{LF}, 10 m x 10 m grid, auxiliary electrodes in the same direction.

C. Impulse impedance (Z_P) and ground resistance (R_{LF}) for 5 m x 5 m grid with auxiliary electrodes in orthogonal

Fig. 13 shows, by way of illustration, a voltage *v(t)* and current *i(t)* waveforms captured when *dA* = 5*D* e *dP* = 0.6 *dA*. Fig. 14 shows the impulse impedance (Z_P) values.

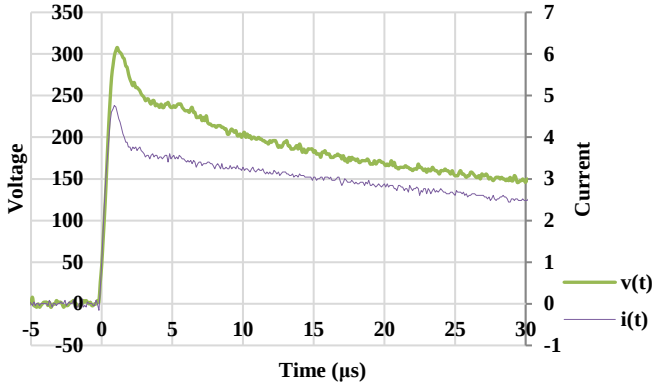

Fig. 13. Voltage *v(t)* and current *i(t)* waveforms for 5 m x 5 m grid, *dA* = 5*D* e *dP* = 0.6 *dA*.

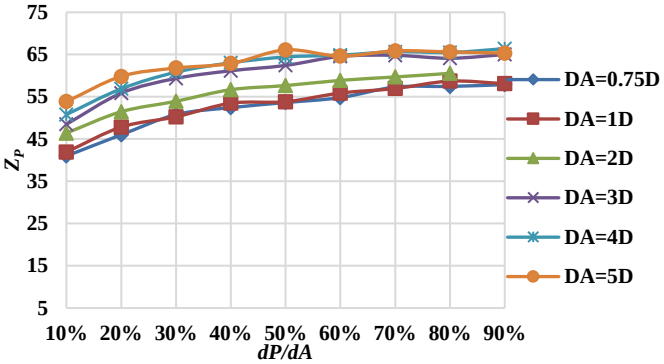

Fig. 14. Impulse impedance Z_P, 5 m x 5 m grid auxiliary electrodes in orthogonal.

In this same measurement setup, Fig. 15 shows the ground resistance values (R_{LF}).

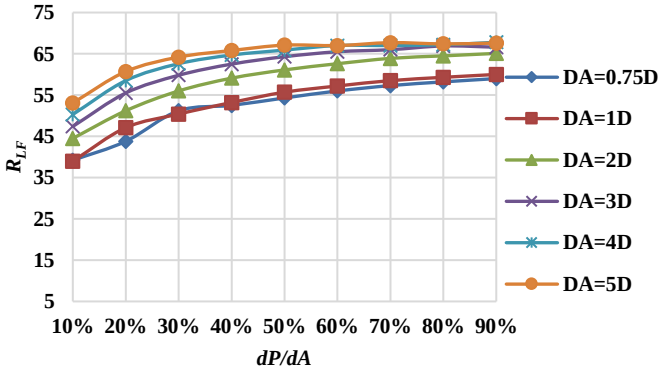

Fig. 15. Ground resistance R_{LF}, 5 m x 5 m grid, auxiliary electrodes in orthogonal.

D. Impulse impedance (Z_P) and ground resistance (R_{LF}) for 10 m x 10 m grid with auxiliary electrodes in orthogonal

Fig. 16 shows, by way of illustration, a voltage *v(t)* and current *i(t)* waveforms captured when *dA* = 5*D* e *dP* = 0.6 *dA*. Fig. 17 shows the impulse impedance (Z_P) values.

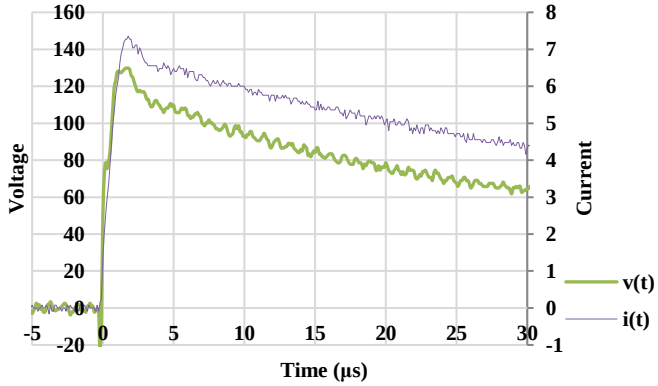

Fig. 16. Voltage *v(t)* and current *i(t)* waveforms for 10 m x 10 m grid, *dA* = 5*D* e *dP* = 0.6 *dA*.

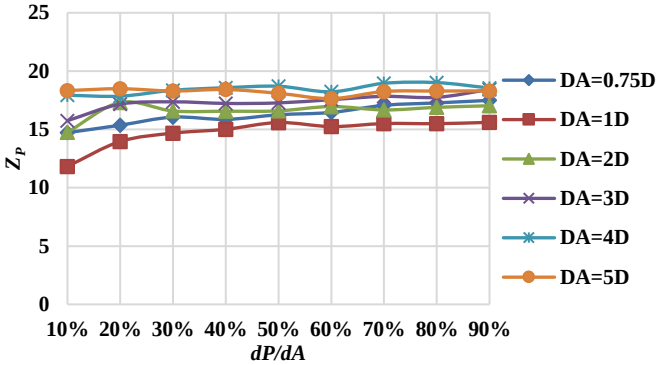

Fig. 17. Impulse impedance Z_P, 10 m x 10 m grid auxiliary electrodes in orthogonal.

In this same measurement setup, Fig. 18 shows the ground resistance values (R_{LF}).

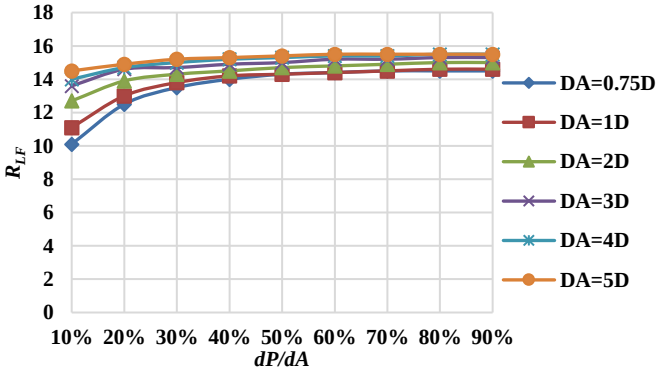

Fig. 18. Ground resistance R_{LF}, 10 m x 10 m grid, auxiliary electrodes in orthogonal.

E. Analysis and discussion of results

1) Ground resistance R_{LF}: The R_{LF} measurements returned results within the expected, both for auxiliary electrodes in the same direction as orthogonal. Plateau values were obtained when *dP* was near 62% of *dA*, for $dA \geq 4D$. For the other measurements, the plateau does not exist due to the proximity between the auxiliary electrodes and the system under measurement, being necessary the application of some measurement method at reduced distance to obtain the plateau value.

2) Impulse impedance with auxiliary electrodes in the same direction: An analysis of the voltage waveforms of these measurements indicates a rapid and intense peak voltage in the moment of the injection of the surge in the ground grid (Fig. 7 e Fig. 10). This is due to the existence of the effect of the inductive coupling on the measurements with auxiliary electrodes in the same direction. It is also confirmed by the analysis of the impulse impedance values (Fig. 8 e Fig. 11), and there is no plateau in all measurements. Therefore, it is possible to affirm that impedance measurements with electrodes in the same direction were interfered by the inductive coupling between the conductors of the auxiliary electrodes, so that the impulse impedance data are not valid for evaluation of the performance of the ground grids.

3) Impulse impedance with orthogonally arranged auxiliary electrodes: As a way to mitigate the effect of the inductive coupling, impedance measurements with orthogonally arranged auxiliary electrodes have proved to be an efficient solution, with a well-defined plateau for the obtained impulse impedance values. In addition, this solution is extremely feasible from the point of view of field application, since does not present major implementation restrictions. In this way, it is evidenced the necessity of carrying out impulse impedance measurements in this configuration to obtain data of high quality and reliability, what allows a correct evaluation of the performance and safety of the grounding system under test.

V. CONCLUSIONS

The fact of providing a varied set of ground resistance and impulse impedance measurement data, as a function of the distances of *dP* and *dA*, is already in itself a considerable contribution to the study and understanding of measurement methodologies, by allowing the use of these results in other studies in this area.

It is interesting to note that although the methodology of impedance measures appears to be relatively simple and widely diffused in academia, its implementation in the field has proved to be a non-trivial task, as discussed in item III of this paper.

Regarding the problems encountered during the measurements, the effect of the inductive coupling between the conductors of the auxiliary electrodes is highlighted as one of the main problems encountered. Although the theory recommends measurement of resistance and impedance with auxiliary electrodes aligned and arranged in the same direction, the application of this condition in the field presented problems, with deformations in the voltage waveforms and, as a consequence, the impossibility of obtaining correct impulse impedance values. The positioning of these auxiliary electrodes in orthogonal was shown as an effective solution to mitigate this effect, allowing the correct values of impulse impedance of ground grids.

Finally, it is concluded that the main objective of this study is achieved by obtaining and disseminating the data and results, making possible its application in future studies within this research area.

REFERENCES

[1] A. Raizer, V. Coelho, W. Valente Jr. and D. M. Magnus, “A Contribution to the Study of Ground Grids Impulse Impedance, Based on Field Measurements,” XIV SIPDA, 2017.

[2] A. Lima, J. Paulino, W. Boaventura, I. Lopes, M. Guimarães, W. Chisholm, B. Jamali and F. Bologna, “Transient grounding impedance and transient resistivity measurements using a very short current lead,” EPSR, pp. 69-75, 2015.

[3] IEEE Power and Energy Society, “ANSI/IEEE Std 80-2013 - IEEE Guide for Safety in AC Substation Grounding,” Nova York, 2013.

[4] ASSOCIAÇÃO BRASILEIRA DE NORMAS TÉCNICAS, “NBR 15749 - Medição de resistência de aterramento e de potenciais na superfície do solo em sistemas de aterramento,” Rio de Janeiro, 2009.

[5] IEEE Power and Energy Society, “ANSI/IEEE Std 81-2012 - IEEE Guide for Measurement Earth Resistivity, Ground Impedance, and Earth Surface Potentials of a Grounding System,” Nova York, 2012.

[6] C.Wang, T. Takasima, T. Sakuta, and Y. Tsubota, “Grounding resistance measurement using fall-of-potential method with potential probe located in opposite direction to the current probe,” IEEE Trans. Power Delivery, vol. 13, pp. 1128–1135, Oct. 1998.

[7] INTERNATIONAL ELECTROTECHNICAL COMMISSION, “IEC 61000-4-5. Electromagnetic Compatibility (EMC) – Part 4-5: Testing and measurement techniques – Surge immunity test,” Genebra, 2014.

[8] A. Raizer, W. Valente Jr. and V. L. Coelho, “Development of a new methodology for measurements of earth resistance, touch and step voltages within urban substations,” EPSR, pp. 111-118, December 2017.

[9] Google, “Google Earth,” [Online]. Available: https://earth.app.goo.gl/?apn=com.google.earth&ibi=com.google.b612&isi=293622097&ius=googleearth&link=https%3a%2f%2fearth.google.com%2fweb%2f%40-27.68155879,-48.53638437,4.99473372a,154.03897432d,35y,332.18311643h,0t,0r. [Accessed on December 19 2018].

[10] MEGABRAS, “Folheto Técnico MTD-20KWe,” 2018. [Online]. Available: https://www.megabras.com/pt-br/get.php?file=MTD20KWe.pdf. [Accessed on July 27 2018].

[11] Tektronix, “MSO3000 and DPO3000 Series Manual,” [Online]. Available: download.tek.com/manual/071265602web.pdf. [Accessed on May 04 2018].

[12] Tektronix, “P6015A Manual,” [Online]. Available: download.tek.com/manual/070822305.pdf. [Accessed on May 04 2018].

[13] Tektronix, “TCP0020 & TCP2020 Manual,” [Online]. Available: download.tek.com/manual/071300200_web_RevA_0.pdf. [Accessed on May 04 2018].

[14] J. Ma and F. P. Dawalibi, “Influence of Inductive Coupling Between Leads on Ground Impedance Measurements Using the Fall-of-Potential Method,” IEEE TRANSACTIONS ON POWER DELIVERY, pp. 739-743, October 2001.